

## A STUDY ON DRYING CHARACTERISTICS, COLOR, AND VITAMIN C PRESERVATION OF GREEN BANANA SLICES USING A VACUUM HEAT PUMP SYSTEM

Narathip Sujinda<sup>a</sup>, Thanapon Saengsuwan<sup>b</sup>, Natthiya Chaichana<sup>c\*</sup>

<sup>a</sup> Faculty of Agriculture at Kamphaeng Saen, Kasetsart University, Nakornpathom, 73140, Thailand, e-mail: narathip.suj@ku.ac.th, ORCID 0000-0002-6657-3261

<sup>b</sup> Energy Engineering and Electric Technology Program, Faculty of Industrial Technology, Chiang Rai Rajabhat University, Chiang Rai 57100, Thailand, e-mail: thanapon.sae@cr.ru.ac.th, ORCID 0000-0003-1283-5454

<sup>c</sup> Science Program, Faculty of Education, Chiang Rai Rajabhat University, Chiang Rai, 57100, Thailand, e-mail: natthiya.cha@cr.ru.ac.th, ORCID 0009-0009-4309-3255

\* Corresponding author: e-mail: natthiya.cha@cr.ru.ac.th

### ARTICLE INFO

#### Article history:

Received: December 2023

Received in the revised form: April 2024

Accepted: May 2024

#### Keywords:

Thin-layer drying model,

Vacuum heat pump drying,

Green Banana slices,

Vitamin C,

Specific moisture extraction rate

### ABSTRACT

This study aimed to evaluate the characteristics related to the removal of moisture from green banana slices and the effect of the drying conditions on color and vitamin C preservation using a drying system based upon the use of a vacuum heat pump. The green banana slices underwent drying at 40, 50, and 60°C with vacuum pressure levels of 0, 40, and 80 kPa. The average drying time decreased by 18.9% and 32.7% as the vacuum pressure and temperature increased, respectively. Six thin-layer models underwent assessment to explain the kinetic process involved in moisture removal using the vacuum heat pump set to provide differing experimental circumstances, and fitted to experimental data. Results showed that the characteristics of moisture removal from the green banana slices could most appropriately be explained by the Page model. There is an increase in effective moisture diffusivity, which ranged from  $1.1658 \times 10^{-10}$  to  $1.9717 \times 10^{-10} \text{ m}^2 \cdot \text{s}^{-1}$ , with increases in temperature and vacuum pressure. Energy of activation ranged from 15.99 to 19.73  $\text{kJ} \cdot \text{mol}^{-1}$ , which was explained by an exponential expression based on the Arrhenius models. The drying temperature of 50°C under a vacuum pressure of 80 kPa could preserve the vitamin C content by a maximum of 55.9%, which is the optimal drying condition for obtaining good product quality.

## Introduction

Bananas are one of the most widely consumed fruits globally due to their delicious taste and nutritional value. Also, it is the cheapest and most energy-dense fruit (Al-Dairi et al., 2023; Li, 2023). In the green stage, bananas offer several health benefits due to their unique nutrient profile. They are a rich source of resistant starch, a specific kind of carbohydrate that

is resistant to being digested in the small intestine and functions as a prebiotic to encourage the development of good gut bacteria. Many health benefits have been associated with resistant starch, including enhanced insulin sensitivity, lower blood sugar levels, and a decreased risk of colon cancer. In addition, green bananas are an outstanding source of vitamin C, an antioxidant that protects against cellular damage and boosts the immune system (Mohapatra et al., 2010; Falcomer et al., 2019; Riquette et al., 2019). As a consequence of the amounts of water contained therein, however, they are highly perishable and require proper preservation techniques to extend their shelf life.

One highly effective approach used to preserve fruit is to dry it, thus removing moisture and inhibiting microbial growth (Seyedabadi, 2017). A number of studies have examined heat pump, hot air, freezing, and vacuum methods to enhance the outcomes when fruit is dried in terms of fruit quality, and to improve the efficiency of energy usage in such procedures. Among numerous drying techniques, heat pump drying is gaining popularity due to its capacity to preserve product quality while attaining a high drying rate with minimal energy use (Colak, 2009). Drying with a heat pump offers enhanced efficiency in terms of energy usage, while simultaneously permitting the regulation of both air humidity and temperature, which makes it particularly well-suited for drying edible crops which might be easily damaged by a lack of temperature control, since it is possible to carry out the process at greatly reduced temperatures (Fan et al., 2004; Hii et al., 2012; Minea, 2013; Yang et al., 2013; Zielinska et al., 2013). According to several studies, agricultural products that are dried with a heat pump drying system are demonstrated to have superior color and flavor qualities to those that are dried with a typical hot air dryer (Prasertsan and Saen-saby, 1998; Teeboonma et al., 2003; Soponronnarit et al., 2007).

A significant amount of research in the literature has been carried out on bananas that have been dried using different kinds of drying via heat pumps. Tunckal and Doymaz in 2020, examined the drying characteristics of banana slices using a drying system based on heat pumps for which the cycle was closed. There was a reduction in the time taken for moisture removal with rising temperature. The statistical analysis revealed that the model proposed by Midilli et al. offered the best fit, generating values for effective moisture diffusivity between  $1.12 \times 10^{-10}$  and  $1.64 \times 10^{-10} \text{ m}^2 \cdot \text{s}^{-1}$ . Accordingly, effective moisture diffusivity rose as the drying temperature increased. Calculation of the energy of activation energy revealed a value of  $51.45 \text{ kJ} \cdot \text{mol}^{-1}$  (Tunckal and Doymaz, 2020). Singh et al. in 2020, evaluate the heat pump drying system performance across four different modes of operation for drying two mm-thick banana chips: conventional, infrared-assisted, solar-assisted, and solar-infrared-assisted heat pump drying. The study demonstrates that integrating multiple drying approaches, including solar, infrared, and heat pumps, can be combined to create a unified approach to accelerate banana chip drying (Singh et al., 2020). In a recent study concerning the drying behavior associated with slices of banana, Meng et al. in 2022 demonstrated that heat pump-electrohydrodynamic combination drying increases drying rates, decreases drying durations by at least 40 minutes, and reduces energy consumption by at least 18%. The diffusion coefficient increases as the voltage increases, whereas the activation energy decreases (Meng et al., 2022).

In the literature, studies involving the drying characteristics of green banana slices using the vacuum heat pump approach have yet to be published. Thus, this research aimed to investigate the effects of temperature and vacuum pressure upon the drying behavior which

results from this heat pump method, and the quality of the green banana slices after drying, fitting the moisture removal data to six models which describe the thin-layer drying process. This allows the calculation of activation energy, effective moisture diffusivity, and specific moisture extraction ratio to evaluate drying system performance as well as the analysis of vitamin C preservation for the evaluation of drying system performance in terms of product quality.

## **Materials and Methods**

### **Sample preparation**

The source of the green banana (*Musa sapientum* L.) samples was a Thai banana plantation. Peeling of the green bananas was followed by washing, before they were longitudinally cut to produce slices with a thickness of 4 mm. These slices were  $100\pm 2$  mm long, and  $25\pm 2$  mm wide, and were then used for subsequent experimentation. The initial moisture content of banana slices was  $65\pm 1$  % wet basis.

### **Vacuum heat pumps**

The laboratory-scale vacuum heat pump system (VHPD) for drying underwent development using a 1.1 kW heat pump in order to provide the drying chamber with heat, along with a 0.7 kW dual-stage rotary vane vacuum pump which served to regulate the pressure within the chamber. A schematic diagram of the vacuum heat pump dryer employed in the current study can be seen in Figure 1. The dryer had three principal elements: the VHPD cavity, heat pump system, and vacuum pump. The green banana slices were put on the tray located within the VHPD cavity for the duration of the VHPD procedure. Monitoring of real-time sample weight loss required the use of a Snug 3 load cell model (Jadever Scale Co., Ltd., Taiwan), which could be positioned within the VHPD cavity located beneath the tray. Then a load cell signal was transmitted to a computer to calculate the moisture content. The heat pump system ran ceaselessly, ensuring a stable temperature in the VHPD cavity. The supply of hot refrigerant to the internal heat pump condenser was controlled by a solenoid valve, which allowed the control of the drying temperature. The role of the solenoid valve was to open or close in response to the temperature moving above or below the required level. The temperature was monitored by a type-K thermocouple positioned at a height of 50 mm over the tray. The temperature differential separating higher and lower specified settings measured  $2^{\circ}\text{C}$ . Inside the VHPD chamber, vapor was produced from the samples during the VHPD process. A vacuum pump pulled the vapor from the drying chamber before condensing it inside the moisture trap.

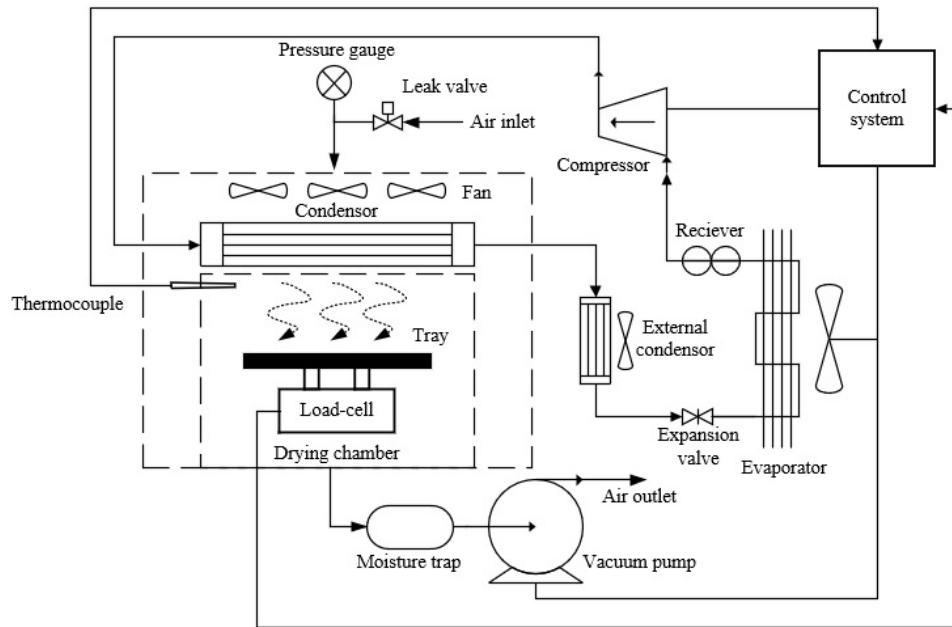


Figure 1. Schematic illustration of the laboratory-scaled VHPD system

### Vacuum heat pump drying (VHPD) experiment

The VHPD was carried out by drying  $400 \pm 0.1$  g of green banana slices using temperatures set to 40, 50, and 60°C under constant pressures of 40, 80 kPa, and drying without the vacuum (0 kPa). The collected real-time weight of the samples was used for the determination of the moisture content levels in real time. The VHPD activity proceeded to the point where the green banana slice moisture content determined in real time was found to be  $10 \pm 1\%$  (the end-point of the process). Drying efficiency was determined by analyzing both the drying curve and the rate of drying for bananas. Some dried banana slices were packed into the aluminum foil bag for further quality assessment. The experiment was performed in triplicate.

### Vacuum heat pump drying characterization

The kinetics models were examined to characterize VHPD. A wet basis was employed to represent material moisture content, and the moisture ratio (MR) was calculated using Equation (1).

$$MR = \frac{M_t - M_e}{M_i - M_e} \quad (1)$$

The moisture ratio is given as  $MR$ ;  $M_i$  and  $M_t$  serve as the respective starting moisture content and content measured at the time  $t$ , while  $M_e$  represents the moisture content at equilibrium. Drying curves ( $MR$  vs. time) could then be applied for the chosen models for dehydrating thin layers, including the Newton (Kaleta and Górnicki, 2010), Page (Arumuganathan et al., 2009), Henderson and Pabis (Kaleta and Górnicki, 2010), Midilli et al. (Midilli et al., 2002), Simplified Fick's diffusion (Demir et al., 2004), and Logarithmic (Xanthopoulos et al., 2007).

Model parameters could be determined via non-linear analysis on the basis of the Levenberg-Marquardt algorithm.  $R^2$  (coefficient of determination),  $RMSE$  (root mean square error), and  $SSE$  (sum of squared error) when comparing predicted and measured moisture values served as indicators of the fit's quality (Torki-Harchegani et al., 2016). The following formulas can be used to calculate  $R^2$ ,  $RMSE$ , and  $SSE$ :

$$R^2 = 1 - \frac{\sum_{i=1}^n (MR_{exp.i} - MR_{pre.i})^2}{\sum_{i=1}^n (MR_{exp.i} - \overline{MR})^2} \quad (2)$$

$$RMSE = \left[ \frac{1}{n} \sum_{i=1}^n (MR_{pre.i} - MR_{exp.i})^2 \right]^{0.5} \quad (3)$$

$$SSE = \frac{1}{n} \sum_{i=1}^n (MR_{exp.i} - MR_{pre.i})^2 \quad (4)$$

#### Moisture diffusivity ( $D$ ) estimation

Fick's second law diffusion model determined moisture transfer during the VHPD process. Moisture transport was obtained by assuming a slab body in the case of the slices of banana. These are as follows: (1) the initial moisture is distributed uniformly across the entire sample mass, while (2) external resistance and contraction appear negligible during the entire drying procedure. The authors considered all banana slices to be an infinite slab and utilized Fick's second law of diffusion. Continuous moisture diffusivity was first demonstrated via an equation developed by Crank in 1979 (Crank, 1979). This is demonstrated by the following Equation (5):

$$MR = \frac{8}{\pi^2} \exp\left(\frac{-\pi^2 D t}{L^2}\right) \quad (5)$$

$D$  indicates moisture diffusivity ( $m^2 \cdot s^{-1}$ ),  $L$  serves as the thickness of the banana slices in m, while  $t$  indicates the time taken for the drying process (s). Moisture diffusivity ( $D$ ) could be obtained by simplifying Equation 5 to a logarithmic format before evaluating the Fourier number,  $F_0 = D \cdot t \cdot (L^2)^{-1}$ , as shown in Equation (6). Thus, Equation (5) can be rewritten as Equations (6) to (8):

$$\ln(MR) = \ln \frac{8}{\pi^2} - \pi^2 F_0 \quad (6)$$

$$F_0 = -0.10124 \ln(MR) - 0.02134 \quad (7)$$

$$D = \frac{F_0 L^2}{t} \quad (8)$$

### Estimation of activation energy

An equation of the Arrhenius type can be assumed to describe how the effective moisture diffusivity and air temperature are related (Onwude et al., 2016). This equation is expressed as shown below:

$$D_{eff} = D_0 \exp\left(-\frac{E_a}{R(T+273.15)}\right) \quad (9)$$

For determining  $E_a$ , Equation (9) can be written as follows

$$\ln(D_{eff}) = \ln(D_0) - \left(\frac{E_a}{R}\right) \left(\frac{1}{(T+273.15)}\right) \quad (10)$$

$D_0$  represents the pre-exponential factor ( $\text{m}^2 \cdot \text{s}^{-1}$ ), energy of activation is given by  $E_a$  ( $\text{kJ mol}^{-1}$ ), while temperature is shown as  $T$  ( $^{\circ}\text{C}$ ), and  $R$  is used to indicate the universal gas constant ( $\text{kJ} \cdot (\text{mol} \cdot \text{K})^{-1}$ ).

### Consumption of energy and rate of specific moisture extraction

Energy usage associated with the vacuum pump and heat pump equipment was used to calculate the total consumption of energy related to the VHPD procedure. Energy consumption could be logged through the use of a PZEM-061 power meter (Ningbo Peacefair Electronic Co., Ltd., China). The kWh value obtained from the power meter is then converted to MJ, since  $1 \text{ kWh} = 3.6 \text{ MJ}$ .

An indicator of how effective the drying procedure is in terms of energy consumption is the SMER (specific moisture extraction rate). SMER can be calculated by taking the amount of moisture extracted (in kilograms of moisture) divided by the amount of energy used (in kilowatt-hours). The SMER was calculated as follows (Sujinda et al., 2021):

$$SMER = \frac{\text{Kilograms of removal moisture}}{\text{Energy consumption}} \quad (11)$$

### Color analysis

The pigmentation of the banana slices was quantified using a MiniScan XE Plus spectrophotometer (Hunter Associates Laboratory, Inc., USA). The calibration of the spectrophotometer was performed by utilizing a standard white and black plate. The configuration of the light source utilized in the experiment was D65/10°. In order to ascertain the color, the sample was subjected to random illumination on the surface of the banana. The color characteristics were documented using the CIE  $L^* \text{-} a^* \text{-} b^*$  scale, wherein  $L^*$  denoted brightness and  $a^*$  represented the chromatic element ranging from green to red, while  $b^*$  represented the chromatic element ranging from blue to yellow. The color analysis was repeated three times for each treatment.

### Vitamin C preservation rate

The rate of vitamin C preservation (calculated by dividing the vitamin C content prior to drying by the content level after completion of the drying procedure) could be employed as a means of describing the alteration in the nutritional composition during the course of the moisture removal procedure, because vitamin C is sensitive to heat. At identical final moisture content levels, drying trials were performed at various temperatures (40, 50, and 60°C) and vacuum pressures (0, 40, and 80 kPa). Application of the high-performance liquid chromatography (HPLC) method allowed the vitamin C content to be determined. The trial was repeated three times. The data were converted to micrograms per 100 grams of solids, whereupon the rate of vitamin C preservation could be determined.

### Data analysis

The data were analyzed for the Analysis of Variance (ANOVA) by using SPSS 24.0 (SAS Institute Inc., USA). Comparison of the mean was conducted through the application of Duncan's new multiple range test, with findings indicating significant differences ( $p < 0.05$ ) in the data.

## Results and Discussion

### Kinetics of drying

To investigate some effects of both the temperature and the vacuum pressure upon the kinetic characteristics of the drying process, various drying conditions, including temperatures of 40, 50, and 60°C along with vacuum pressures measuring 0, 40, and 80 kPa, were utilized. A drying curve can be constructed to indicate the drying kinetics by describing the way moisture levels and drying times are associated, as shown in Figure 2, and the relationship connecting the rate of drying and the moisture content, as shown in Figure 3.

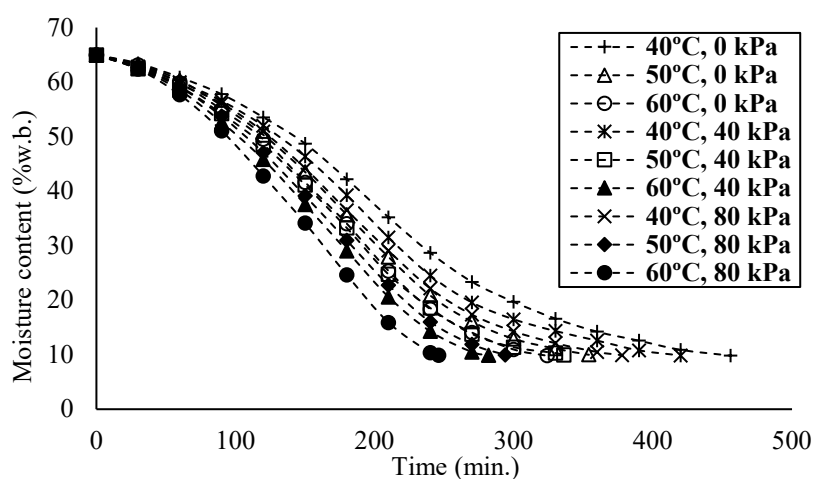


Figure 2. The drying curve of green banana slices under various VHPD conditions

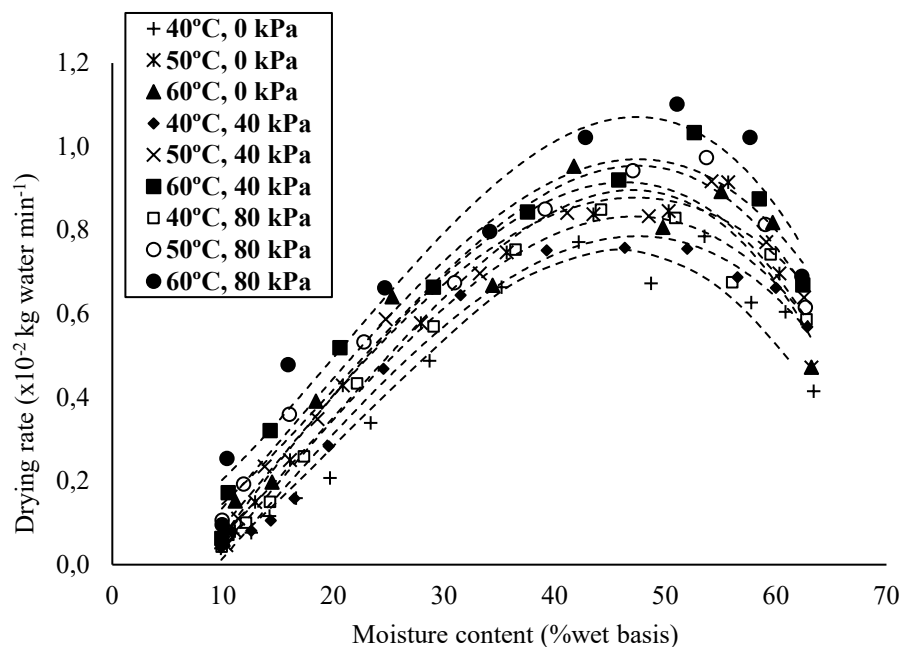


Figure 3. The curve representing the rate of drying for green banana slices under various VHPD conditions.

Figures 2 and 3 represent the drying rate and drying time range from  $0.4$  to  $1.1 \times 10^{-2} \text{ kg}_{\text{water}} \text{ min}^{-1}$  and  $246$  to  $456$  minutes, respectively. The drying time decreased as the temperature and vacuum pressure levels increased, resulting in an increased drying rate. Consistent with previous research on drying Jinda chili (Artnaseaw et al., 2010), carrot and pumpkin (Arévalo-Pinedo and Murr, 2007), the experimental results indicate that there is a rise in the rate of drying as the temperature also rises. The maximal rate of drying and minimum drying time are  $1.1 \times 10^{-2} \text{ kg}_{\text{water}} \text{ min}^{-1}$  and  $t = 246$  min, respectively, at  $60^\circ\text{C}$  and  $80 \text{ kPa}$  of vacuum pressure. The drying curves in Figure 2 appear commonplace for related edible plant crops. As drying time went on, there was an exponential reduction in the level of moisture present. As assumed, the temperature and vacuum pressure significantly impacted the reduction of the moisture content of green banana slices. There was a considerable reduction in the time taken for moisture removal when the temperature and vacuum pressure rose, according to our results. Figure 2 displays the time taken in order to achieve the terminal moisture level for the slices of green banana. The mean time for moisture removal was reduced by  $18.9\%$  while vacuum pressure rose to  $80 \text{ kPa}$  from  $0$  at the same drying temperature and by  $32.7\%$  with rising temperature to  $60^\circ\text{C}$  from  $40^\circ\text{C}$  while maintaining the same vacuum pressure level.

Drying theory divides drying mechanisms into three zones: beginning (drying rate increase), constant rate, and falling rate (Ratti, 2008). This experiment found an initial zone



between commencement of drying and the highest rate of drying of roughly zero to 45 minutes. As temperature increased, moisture content of this zone was gradually reduced because the sample temperature was lower than the targeted drying temperature, and conduction transferred heat from the sample surface to the inner part to evaporate the sample moisture. Our vacuum pump pulled out the vapor from the drying chamber through the leak valve. The rate of drying tends to rise until it reaches the point at which the partial vapor pressure exerted upon the surface of the sample achieves saturation. Thereafter, the rate of drying slows rapidly until moisture content reaches the final moisture content (10% wet basis). Then the drying process ended. However, in this study, the constant rate zone was not able to be identified in our investigation, which is consistent with the findings of Arévalo-Pinedo and Murr in 2007 dried carrot and pumpkin using vacuum drying (Arévalo-Pinedo and Murr, 2007), Jena and Das in 2007 dried of coconut presscake using vacuum drying (Jena and Das, 2007), and Artnaseaw et al. in 2010 dried mushroom and Jinda chili using vacuum heat pump drying (Artnaseaw et al., 2010). Thus, most investigations were conducted within the zone of the falling rate, as was the case in earlier research discussed previously, indicating no constant rate of drying for agricultural products (Jayatunga and Amarasinghe, 2019).

### Evaluation of the models

The Page model was demonstrated to provide the best fit when considering the data obtained from experiments using the VHPD of green banana slices, since it provided the greatest  $R^2$  value (coefficient of determination), and smallest  $SSE$  (sum of squared error) and  $RMSE$  (root mean squared error) results. The statistical results and coefficients of the Page model can be seen in Table 1. The  $R^2$ ,  $RMSE$ , and  $SSE$  results generated using this particular model showed variation ranging respectively from 0.9969 to 0.9996, 0.0038 to 0.0202, and 0.00001 to 0.00041. Additionally, the Page model was validated by comparing the predicted and experimental moisture ratios for each drying conditions. Figure 4 shows the Page model efficacy under various temperatures or vacuum pressure levels. As demonstrated, predicted moisture ratios typically form clusters around a line set at  $45^\circ$ , suggesting that the model is able to explain the sample drying characteristics in a suitable manner.

Table 1.  
*Statistical findings and Page model coefficients for temperature and vacuum pressure.*

Model	T (°C)	P (kPa)	Parameters	$R^2$	RMSE	SSE
Newton	40	0	$k = 5.38 \times 10^{-3}$	0.9778	0.0759	0.00577
		40	$k = 5.89 \times 10^{-3}$	0.9789	0.0687	0.00472
		80	$k = 6.25 \times 10^{-3}$	0.9781	0.0688	0.00474
	50	0	$k = 6.35 \times 10^{-3}$	0.9750	0.0743	0.00552
		40	$k = 6.84 \times 10^{-3}$	0.9792	0.0655	0.00429
		80	$k = 7.08 \times 10^{-3}$	0.9748	0.0666	0.00443
	60	0	$k = 6.59 \times 10^{-3}$	0.9729	0.0668	0.00446
		40	$k = 7.46 \times 10^{-3}$	0.9766	0.0580	0.00336
		80	$k = 8.12 \times 10^{-3}$	0.8703	0.0549	0.00302

Model	T (°C)	P (kPa)	Parameters	R <sup>2</sup>	RMSE	SSE
Page	40	0	$k = 3.59 \times 10^{-4}$ , $n = 1.510$	0.9972	0.0202	0.00041
		40	$k = 5.05 \times 10^{-4}$ , $n = 1.470$	0.9969	0.0201	0.00040
		80	$k = 4.83 \times 10^{-4}$ , $n = 1.495$	0.9977	0.0169	0.00029
	50	0	$k = 2.84 \times 10^{-4}$ , $n = 1.608$	0.9990	0.0064	0.00004
		40	$k = 4.84 \times 10^{-4}$ , $n = 1.522$	0.9988	0.0088	0.00005
		80	$k = 4.36 \times 10^{-4}$ , $n = 1.557$	0.9996	0.0064	0.00004
	60	0	$k = 3.15 \times 10^{-4}$ , $n = 1.598$	0.9991	0.0087	0.00008
		40	$k = 5.25 \times 10^{-4}$ , $n = 1.533$	0.9996	0.0057	0.00003
		80	$k = 5.06 \times 10^{-4}$ , $n = 1.567$	0.9995	0.0038	0.00001
Henderson and Pabis	40	0	$k = 5.95 \times 10^{-3}$ , $a = 1.110$	0.9726	0.0622	0.00387
		40	$k = 6.43 \times 10^{-3}$ , $a = 1.096$	0.9743	0.0579	0.00335
		80	$k = 6.83 \times 10^{-3}$ , $a = 1.096$	0.9728	0.0583	0.00340
	50	0	$k = 7.02 \times 10^{-3}$ , $a = 1.109$	0.9683	0.0619	0.00384
		40	$k = 7.45 \times 10^{-3}$ , $a = 1.093$	0.9739	0.0557	0.00310
		80	$k = 7.75 \times 10^{-3}$ , $a = 1.095$	0.9679	0.0569	0.00324
	60	0	$k = 7.29 \times 10^{-3}$ , $a = 1.107$	0.9653	0.0563	0.00317
		40	$k = 8.12 \times 10^{-3}$ , $a = 1.092$	0.9702	0.0499	0.00249
		80	$k = 8.84 \times 10^{-3}$ , $a = 1.092$	0.8549	0.0477	0.00227
Midilli et al.	40	0	$k = 1.39 \times 10^{-4}$ , $n = 1.705$ , $a = 0.984$ , $b = 1.20 \times 10^{-4}$	0.9963	0.0295	0.00099
		40	$k = 1.93 \times 10^{-4}$ , $n = 1.668$ , $a = 0.977$ , $b = 1.16 \times 10^{-4}$	0.9960	0.0226	0.00082
		80	$k = 2.10 \times 10^{-4}$ , $n = 1.667$ , $a = 0.978$ , $b = 1.07 \times 10^{-4}$	0.9911	0.0217	0.00084
	50	0	$k = 1.80 \times 10^{-4}$ , $n = 1.707$ , $a = 0.988$ , $b = 1.07 \times 10^{-4}$	0.9861	0.0297	0.00094
		40	$k = 3.10 \times 10^{-4}$ , $n = 1.616$ , $a = 0.984$ , $b = 0.89 \times 10^{-4}$	0.9788	0.0294	0.00085
		80	$k = 3.86 \times 10^{-4}$ , $n = 1.579$ , $a = 0.992$ , $b = 0$	0.9896	0.0372	0.00073
	60	0	$k = 2.11 \times 10^{-4}$ , $n = 1.683$ , $a = 0.989$ , $b = 0.69 \times 10^{-4}$	0.9467	0.0388	0.00095
		40	$k = 4.38 \times 10^{-4}$ , $n = 1.569$ , $a = 0.990$ , $b = 0.17 \times 10^{-4}$	0.9446	0.0351	0.00082
		80	$k = 4.54 \times 10^{-4}$ , $n = 1.587$ , $a = 0.992$ , $b = 0$	0.9420	0.0433	0.00091
Simplified Fick's diffusion	40	0	$k = 3.49 \times 10^{-3}$ , $a = 1.263$ , $b = 1.00 \times 10^{-4}$	0.9797	0.0559	0.00312
		40	$k = 3.95 \times 10^{-3}$ , $a = 1.236$ , $b = 1.00 \times 10^{-4}$	0.9819	0.0499	0.00249
		80	$k = 3.91 \times 10^{-3}$ , $a = 1.291$ , $b = 0.99 \times 10^{-4}$	0.9833	0.0466	0.00217
	50	0	$k = 3.47 \times 10^{-3}$ , $a = 1.417$ , $b = 0.99 \times 10^{-4}$	0.9822	0.0479	0.00229
		40	$k = 4.16 \times 10^{-3}$ , $a = 1.311$ , $b = 0.99 \times 10^{-4}$	0.9857	0.0416	0.00173
		80	$k = 3.29 \times 10^{-3}$ , $a = 1.600$ , $b = 0.99 \times 10^{-4}$	0.9884	0.0350	0.00123

Model	T (°C)	P (kPa)	Parameters	R <sup>2</sup>	RMSE	SSE
Logarithmic	60	0	k = 3.05x10 <sup>-3</sup> , a = 1.604, b = 0.99x10 <sup>-4</sup>	0.9851	0.0379	0.00143
		40	k = 3.64x10 <sup>-3</sup> , a = 1.534, b = 0.99x10 <sup>-4</sup>	0.9898	0.0296	0.00877
		80	k = 3.39x10 <sup>-3</sup> , a = 1.721, b = 0.99x10 <sup>-4</sup>	0.9914	0.0247	0.00610
	40	0	k = 5.95x10 <sup>-3</sup> , a = 1.100, b = 0	0.9726	0.0622	0.00387
		40	k = 6.20x10 <sup>-3</sup> , a = 1.077, b = 0	0.9765	0.0587	0.00345
		80	k = 6.83x10 <sup>-3</sup> , a = 1.096, b = 0	0.9728	0.0583	0.00340
	50	0	k = 7.02x10 <sup>-3</sup> , a = 1.109, b = 0	0.9683	0.0620	0.00384
		40	k = 7.45x10 <sup>-3</sup> , a = 1.093, b = 0	0.9739	0.0557	0.00310
		80	k = 7.75x10 <sup>-3</sup> , a = 1.092, b = 0	0.9680	0.0569	0.00325
60	0	k = 4.92x10 <sup>-3</sup> , a = 1.058, b = 0	0.9856	0.0346	0.00119	
	40	k = 5.50x10 <sup>-3</sup> , a = 1.044, b = 0	0.9898	0.0277	0.00077	
	80	k = 8.84x10 <sup>-3</sup> , a = 1.092, b = 0	0.9669	0.0477	0.00227	

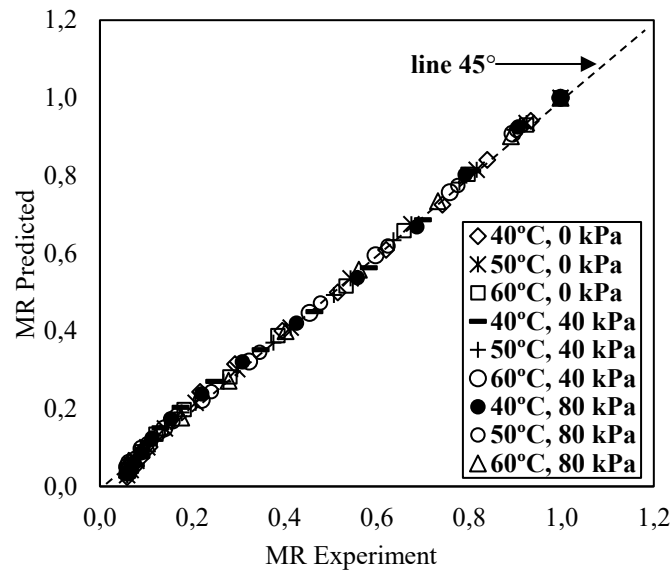


Figure 4. Comparing the predicted and experimental moisture ratios via the Page model for the VHPD of green banana slices at various temperatures and vacuum pressures

### Effective moisture diffusivity and required energy of activation

The effective diffusivity ( $D_{eff}$ ) and activation energy ( $E_a$ ) for the VHPD of green banana slices can be seen in Table 2 for the various temperatures of 40, 50, and 60°C and vacuum pressures measuring 0, 40, and 80 kPa. Values for effective diffusivity ranged between  $1.533 \times 10^{-10}$  and  $1.9757 \times 10^{-10} \text{ m}^2 \cdot \text{s}^{-1}$ , as anticipated for the ranges of drying crops ( $10^{-11}$  to  $10^{-9} \text{ m}^2 \cdot \text{s}^{-1}$ ) and food products ( $10^{-11}$  to  $10^{-6} \text{ m}^2 \cdot \text{s}^{-1}$ ) (Madamba et al., 1996). A rising temperature resulted in greater diffusivity effectiveness since the mass transfer was accelerated (Aghbashlo et al., 2008; Arslan et al., 2010; Meziane, 2011). The greatest  $D_{eff}$  was reached for the drying temperature measuring 60°C with the vacuum pressure at 80 kPa. The findings for the influence of temperature increases concur with earlier research, since increases in drying temperatures lead to lower water viscosity and a concomitant rise in molecular activation, causing greater diffusion of the water molecules within the samples, along with a rise in moisture diffusion (Kaleemullah and Kailappan, 2006; Beigi, 2016). In addition, the vacuum pressure was responsible for moisture transportation, which resulted in rising moisture diffusivity and activation energy. With the heating of moisture inside the slices of green banana, it would be probable that vapor pressure was created within the solid matrix of the samples, resulting in a pressure gradient being formed between the vapor pressure internally and the vacuum pressure externally on the sample surface. Pressure gradients can help in transferring moisture (Datta and Ananteswaran, 2001), increasing moisture diffusivity and the energy needed for activation.  $E_a$  increases as vacuum pressure increases and ranges from 16.47 to 19.60  $\text{kJ} \cdot \text{mol}^{-1}$ , consistent with previous studies ranging from 12 to 110  $\text{kJ} \cdot \text{mol}^{-1}$  in the case of food products (Zogzas et al., 1996).

Table 2.

*Effective moisture diffusivity, specific moisture extraction rate, energy consumption, total drying time, and activation energy for VHPD.*

$P$ (kPa)	$T$ (°C)	$D_{eff}$ ( $\times 10^{-10} \text{ m}^2 \cdot \text{s}^{-1}$ )	$E_a$ ( $\text{kJ} \cdot (\text{mol} \cdot \text{K})^{-1}$ )	EC (MJ)	SMER ( $\text{kg}_{\text{water}} \cdot \text{kWh}^{-1}$ )	Drying time (min.)
0	40	$1.1533 \pm 0.0122^a$		$6.77 \pm 0.07^a$	$0.130 \pm 0.001^a$	$451 \pm 4^a$
	50	$1.4631 \pm 0.0040^b$	$16.47 \pm 0.41^a$	$5.27 \pm 0.45^b$	$0.167 \pm 0.002^b$	$351 \pm 3^b$
	60	$1.6844 \pm 0.0045^c$		$4.86 \pm 0.09^c$	$0.181 \pm 0.004^c$	$324 \pm 6^c$
40	40	$1.1653 \pm 0.0039^d$		$8.55 \pm 0.11^d$	$0.103 \pm 0.001^d$	$426 \pm 5^d$
	50	$1.5733 \pm 0.0071^e$	$18.29 \pm 0.14^b$	$6.75 \pm 0.08^a$	$0.130 \pm 0.001^a$	$336 \pm 4^e$
	60	$1.7736 \pm 0.0054^f$		$5.68 \pm 0.03^c$	$0.155 \pm 0.001^c$	$283 \pm 2^f$
80	40	$1.2582 \pm 0.0057^c$		$7.61 \pm 0.11^f$	$0.116 \pm 0.002^f$	$378 \pm 5^g$
	50	$1.6401 \pm 0.0029^f$	$19.60 \pm 0.12^c$	$5.97 \pm 0.16^g$	$0.147 \pm 0.004^g$	$297 \pm 8^h$
	60	$1.9757 \pm 0.0036^g$		$4.92 \pm 0.09^c$	$0.179 \pm 0.003^c$	$245 \pm 5^i$

Note: Values indicated by letters in superscript from the same column show no mutually significant difference ( $p \geq 0.05$ ).

### Consumption of energy and product quality

Efficiency for EC (energy consumption) and SMER (specific moisture extraction rate) was assessed. Greater SMER values are indicative of greater drying efficiency (Stawreberg

and Nilsson, 2010). The energy consumption decreased with increased drying temperature due to reduced drying time. Still, it increased with an increase in the vacuum pressure levels due to a vacuum pump being used, even though the drying time showed a reduction. Although it was clear that the drying temperature of 60°C without vacuum pressure (0 kPa) resulted in the lowest EC of 4.86 MJ and the highest SMER of 0.181 kg<sub>water</sub>·kWh<sup>-1</sup> (Table 2). On the other hand, the energy consumption and SMER of the drying temperature of 60°C with 80 kPa vacuum pressure was not significantly different ( $P \geq 0.05$ ) from that of the temperature of 60°C without vacuum pressure (0 kPa), but the drying temperature of 60°C with 80 kPa vacuum pressure provided better product quality (Table 3 and Figure 5).

Table 3.  
Result of dried green banana slice color analysis.

<i>P</i> (kPa)	<i>T</i> (°C)	<i>L</i> *	<i>a</i> *	<i>b</i> *
0	40	75.1 ± 2.5 <sup>a</sup>	3.4 ± 0.2 <sup>a</sup>	19.3 ± 0.8 <sup>a</sup>
	50	72.2 ± 1.2 <sup>a</sup>	3.9 ± 0.3 <sup>b</sup>	18.0 ± 0.9 <sup>b</sup>
	60	68.0 ± 1.9 <sup>b</sup>	4.2 ± 0.4 <sup>b</sup>	17.4 ± 0.7 <sup>b</sup>
40	40	88.7 ± 0.7 <sup>c</sup>	2.8 ± 1.5 <sup>c</sup>	12.7 ± 0.5 <sup>c</sup>
	50	86.0 ± 1.2 <sup>d</sup>	3.1 ± 0.1 <sup>c</sup>	11.5 ± 0.5 <sup>d</sup>
	60	84.5 ± 1.3 <sup>c</sup>	3.1 ± 0.1 <sup>c</sup>	10.9 ± 0.7 <sup>d</sup>
80	40	88.4 ± 0.7 <sup>c</sup>	2.8 ± 0.2 <sup>c</sup>	12.6 ± 0.5 <sup>c</sup>
	50	85.3 ± 1.2 <sup>d</sup>	3.1 ± 0.2 <sup>c</sup>	11.6 ± 0.3 <sup>d</sup>
	60	83.8 ± 0.9 <sup>e</sup>	3.2 ± 0.1 <sup>c</sup>	10.7 ± 0.5 <sup>d</sup>

Note: Values indicated by letters in superscript from the same column show no mutually significant difference ( $p \geq 0.05$ ).

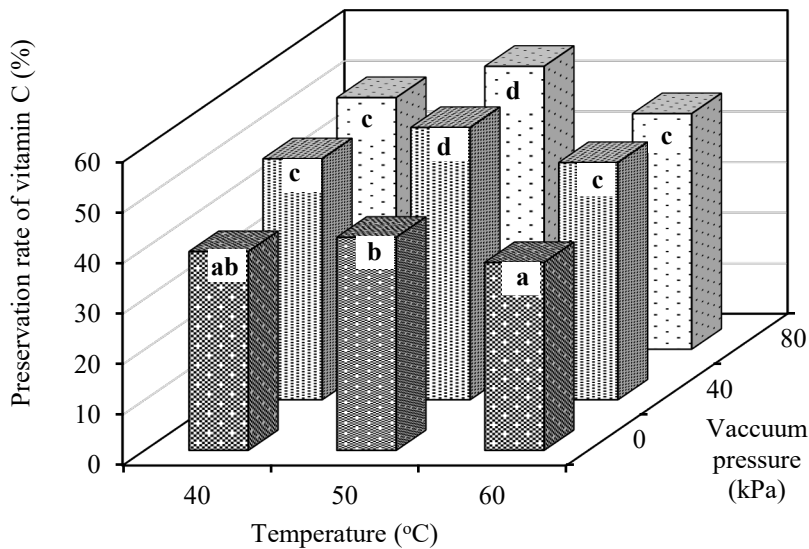


Figure 5. Preservation rate of vitamin C at different drying condition

Note: Values indicated by letters in superscript from the same row show no mutually significant difference ( $p \geq 0.05$ ).

For the purpose of examining the influence of VHPD upon the quality of the product, trials were performed for various drying temperatures and vacuum pressure levels while holding all other values constant. During the trials, the color and preservation rate of vitamin C was employed as a baseline from which to make the assessments.

The two-way analysis of variance revealed a significant effect of drying temperature and vacuum pressure on the color and vitamin C preservation of the dried green banana ( $p < 0.05$ ). The findings presented in Table 3 demonstrate a statistically significant reduction in  $L^*$ , accompanied by an elevation in both  $a^*$  and  $b^*$  values under VHPD without vacuum pressure and an increase in the curing temperature. These results suggest that the green banana slices exhibited a progressively darker color as the drying temperature was raised. Higher temperatures accelerate chemical reactions, which include enzymatic browning and non-enzymatic browning. These reactions involve the breakdown of natural compounds in the banana, which reduces the overall brightness of the dried banana, causing it to seem darker in color (Swasdi-sevi et al., 2007; Macedo et. al, 2020; Gadhave et. al., 2023). Conversely, alterations in vacuum pressure levels do not influence the phenomenon of color transition. However, the drying conditions without vacuum pressure negatively affected the color of the banana slices compared to other treatments. This indicates that the vacuum can minimize oxidative reactions, which can preserve the banana color due to the vacuum's non-oxygen environment.

Figure. 5, reveals maximum content levels for vitamin C under different drying conditions. Data analysis confirmed the significant difference ( $p \geq 0.05$ ) in the vitamin C preservation rate between drying under atmosphere conditions (0 kPa) and vacuum pressure of 40 kPa and 80 kPa. This is because ascorbic acid reacts significantly with oxygen and oxidizes during drying under atmospheric conditions, thereby decreasing vitamin C content (Lee and Kader, 2000). Thus, drying green banana slices in vacuum conditions can prevent the oxidation of ascorbic acid and preserve the vitamin C content during the drying process more than that of drying under atmospheric conditions. However, there has no significant difference ( $p \geq 0.05$ ) in the vitamin C preservation rate in terms of its relationship with vacuum pressure levels (40 kPa and 80 kPa), although a significant relationship was found with drying temperature ( $p < 0.05$ ). This was most likely due to the low temperature requiring a longer drying time (Table 2), resulting in vitamin C degradation, while high temperature also had the same effect (Rahim et al., 2010; Tchuenchieu et al., 2018; Tincheva, 2019). Moreover, the result of the two-way analysis of the variance of drying temperature and vacuum pressure on the vitamin C preservation of the dried green banana found that the highest preservation rate of the vitamin C content was 55.9% with good color at a drying temperature of 50°C and vacuum pressure of 80 kPa, which is the optimal drying condition for obtaining good product quality.

## Conclusions

The drying behavior for green banana slices was examined using a VHPD system using three varying sets of temperatures and vacuum pressure levels. The time taken for drying declined while the temperature and vacuum pressure rose. Average time for drying decreased by 18.9% while there was a simultaneous rise in vacuum pressure to 80 kPa from 0 at the same drying temperature and by 32.7% with a rise in temperature to 60°C from 40°C while

maintaining the same vacuum pressure level. A total of six thin-layer models were used to analyze the kinetics of the drying process. Data analysis attributed the best fit to the Page model. Values for effective moisture diffusivity values, calculated on the basis of Fick's second law, lay in the range from  $1.533 \times 10^{-10}$  to  $1.9757 \times 10^{-10} \text{ m}^2 \cdot \text{s}^{-1}$  across temperatures from 40°C to 60°C and vacuum pressure levels of 0 to 80 kPa. There was a rise in effective moisture diffusivity as drying temperature and vacuum pressure also increased. An Arrhenius-type calculation determined the activation energy to range between 16.47 and 19.60  $\text{kJ} \cdot \text{mol}^{-1}$ . The drying temperature of 50°C under a vacuum pressure of 80 kPa could preserve the vitamin C content by a maximum of 55.9%, which is the optimal drying condition for obtaining good product quality.

**Author Contributions:** N.S. contributed to development of the theory and performed the experiment computations. He worked out almost all of the technical details, devised equipment, performed experiment, analyzed data, and wrote the manuscript. N.C. contributed to idea sketch of original research. She verified the analytical methods and supervised the project details. T.S. assisted with experimental measurements and contributed to interpretation of the results. He provided critical feedback on manuscript writing.

**Conflicts of Interest:** The authors declare no conflict of interest

**Funding:** This research did not receive any specific grant from funding agencies in the public, commercial, or not-for-profit sectors.

**Acknowledgments:** The authors would like to express appreciation to Kasetsart University and Chiang Rai Rajabhat University for the supports of research facilities.

## References

- Aghbashlo, M., Kianmehr, M. H. & Samimi-Akhijahani, H. (2008). Influence of drying conditions on the effective moisture diffusivity, energy of activation and energy consumption during the thin-layer drying of berberis fruit (Berberidaceae). *Energy Conversion and Management*, 49(10), 2865-2871.
- Al-Dairi, M., Pathare, P. B., Al-Yahyai, R., Jayasuriya, H. & Al-Attabi Z. (2023). Postharvest quality, technologies, and strategies to reduce losses along the supply chain of banana: A review. *Trends in Food Science & Technology*, 134, 177-191.
- Artnaseaw, A., Theerakulpisut, S. & Benjapiyaporn, C. Drying characteristics of Shiitake mushroom and Jinda chili during vacuum heat pump drying. *Food and Bioprocess Processing*, 88(2), 105-114.
- Arévalo-Pinedo, A. & Murr, F. E. X. (2007). Influence of pre-treatments on the drying kinetics during vacuum drying of carrot and pumpkin. *Journal of Food Engineering*, 80(1), 152-156.
- Arumuganathan, T., Manikantan, M., Rai, R., Anandakumar, S. & Khare, V. (2009). Mathematical modelling of drying kinetics of milky mushroom in a bed dryer. *International Agrophysics*, 23(1).
- Arslan, D., Özcan, M. M. & Mengeş, H. O. (2010). Evaluation of drying methods with respect to drying parameters, some nutritional and colour characteristics of peppermint (*Mentha x piperita* L.). *Energy Conversion and Management*, 51(12), 2769-2775.
- Beigi, M. (2016). Hot air drying of apple slices: dehydration characteristics and quality assessment. *Heat and Mass Transfer*, 52(8), 1435-1442.

- Colak, N. & Hepbasli, A. (2009). A review of heat pump drying: Part 1 – Systems, models and studies. *Energy Conversion and Management*, 50(9), 2180-2186.
- Crank, J. (1979). *The mathematics of diffusion*. Oxford: Oxford university press.
- Datta, A. K. & Anantheswaran, R. C. (2001). *Handbook of microwave technology for food application*. Florida: CRC Press.
- Demir, V., Gunhan, T., Yagcioglu, A. & Degirmencioglu, A. (2004). Mathematical modelling and the determination of some quality parameters of air-dried bay leaves. *Biosystems engineering*, 88(3), 325-335.
- Falcomer, A. L., Riquette, R. F. R., de Lima, B. R., Ginani, V. C. & Zandonadi, R. P. (2019). Health benefits of green banana consumption: A systematic review. *Nutrients*, 11(6), 1222.
- Fan, H., Shao, S. & Tian, C. (2004). Performance investigation on a multi-unit heat pump for simultaneous temperature and humidity control. *Applied Energy*, 113, 883-890.
- Gadhawe, R. K., Kaur, R., Das, R., Prasad, K. (2023). Dehydration kinetics of green banana slices, characterization of optimized product based on physicochemical, nutritional, optical, and sensory attributes. *Journal of Applied Biology & Biotechnology*, 11(6), 82-93.
- Hii, C. L., Law, C. L. & Suzannah, S. (2012). Drying kinetics of the individual layer of cocoa beans during heat pump drying. *Journal of Food Engineering*, 108(2), 276-282.
- Jayatunga, G. K. & Amarasinghe, B. M. W. P. K. (2019). Drying kinetics, quality and moisture diffusivity of spouted bed dried Sri Lankan black pepper. *Journal of Food Engineering*, 263, 38-45.
- Jena, S. & Das, H. (2007). Modelling for vacuum drying characteristics of coconut presscake. *Journal of Food Engineering*, 79(1), 92-99.
- Kaleemullah, S. & Kailappan, R. (2006). Modelling of thin-layer drying kinetics of red chillies. *Journal of Food Engineering*, 76(4), 531-537.
- Kaletka, A. & Górnicki, K. (2010). Some remarks on evaluation of drying models of red beet particles. *Energy Conversion and Management*, 51(12), 2967-2978.
- Lee, S. K. & Kader, A. A. (2000). Preharvest and postharvest factors influencing vitamin C content of horticultural crops. *Postharvest Biology and Technology*, 20(3), 207-220.
- Li, Z. (2023). Modeling banana uptake of pesticides by incorporating a peel-pulp interaction system into a multicompartment fruit tree model. *Journal of Hazardous Materials*, 444, 130411.
- Macedo, L. L., Vimercati, W. C., Araújo, C. S., Saraiva, S. H., & Teixeira, L. J. Q. (2020). Effect of drying air temperature on drying kinetics and physicochemical characteristics of dried banana. *Journal of Food Process Engineering*, 43(9), e13451.
- Madamba, P. S., Driscoll, R. H. & Buckle, K. A. (1996). The thin-layer drying characteristics of garlic slices. *Journal of Food Engineering*, 29(1), 75-97.
- Meng, Z., Cui, X., Liu, Y., Hu, R., Du, C., Wang, S. & Zhang, F. (2022). Drying characteristics of banana slices under heat pump-electrohydrodynamic (EHD) combined drying. *Sustainable Energy Technologies and Assessments*, 54, 102907.
- Meziane, S. (2011). Drying kinetics of olive pomace in a fluidized bed dryer. *Energy Conversion and Management*, 52(3), 1644-1649.
- Midilli, A., Kucuk, H. & Yapar, Z. (2002). A new model for single-layer drying. *Drying Technology*, 20(7), 1503-1513.
- Minea, V. (2013). Drying heat pumps – Part II: Agro-food, biological and wood products. *International Journal of Refrigeration*, 36(3), 659-673.
- Mohapatra, D., Mishra, S. & Sutar, N. (2010). Banana and its by-product utilisation: An overview. *Journal of Scientific and Industrial Research*, 69(5), 323-329.
- Onwude, D. I., Hashim, N., Janius, R. B., Nawi, N. M. & Abdan, K. (2016). Modeling the Thin-Layer Drying of Fruits and Vegetables: A Review. *Comprehensive Reviews in Food Science and Food Safety*, 15(3), 599-618.
- Prasertsan, S. & Saen-saby, P. (1998). Heat pump drying of agricultural materials. *Drying Technology*, 16(1-2), 235-250.



- Rahim, M. S. A. A., Salihon, J., Yusoff, M. M., Bakar, I. A. & Damanik, M. R. M. (2010). Effect of Temperature and Time to the Antioxidant Activity in *Plectranthus amboinicus* Lour. *American Journal of Applied Sciences*, 7(9).
- Ratti, C. (2008). *Advances in Food Dehydration*. Florida: CRC Press.
- Riquette, R. F. R., Ginani, V. C., Leandro, E. D. S., de Alencar, E. R., Maldonado, I. R., de Aguiar, L. A., de Souza Acácio, G. M., Mariano, D. R. H. & Zandonadi, R. P. (2019). Do production and storage affect the quality of green banana biomass?. *LWT*, 111, 190-203.
- Seyedabadi, E., Khojastehpour, M. & Abbaspour-Fard, M. H. (2017). Convective drying simulation of banana slabs considering non-isotropic shrinkage using FEM with the Arbitrary Lagrangian–Eulerian method. *International Journal of Food Properties*, 20(sup1), S36-S49.
- Singh, A., Sarkar, J. & Sahoo, R. R. (2020). Experimental performance analysis of novel indirect-expansion solar-infrared assisted heat pump dryer for agricultural products. *Solar Energy*, 206, 907-917.
- Soponronnarit, S., Nathakaranakule, A., Wetchacama, S., Swasdisevi, T. & Rukprang, P. (2007). Fruit drying using heat pump. *International Energy Journal*, 20(1), 39-53.
- Stawreberg, L. & Nilsson, L. (2010). Modelling of specific moisture extraction rate and leakage ratio in a condensing tumble dryer. *Applied thermal engineering*, 30(14-15), 2173-2179.
- Sujinda, N., Varith, J., Shamsudin, R., Jaturonglumert, S. & Chamnan S. Development of a closed-loop control system for microwave freeze-drying of carrot slices using a dynamic microwave logic control. *Journal of Food Engineering*, 302, 110559.
- Sawasdisevi, T., Devahastin, S., Ngamchum, R., & Soponronnarit, S. (2007). Optimization of a drying process using infrared-vacuum drying of Cavendish banana slices. *Songklanakarin Journal of Science and Technology*, 29(3), 809-816.
- Tchuenchieu, A., Essia Ngang, J. J., Servais, M., Dermience, M., Sado Kamdem, S., Etoa, F. X. & Sindic, M. (2018). Effect of low thermal pasteurization in combination with carvacrol on color, antioxidant capacity, phenolic and vitamin C contents of fruit juices. *Food Science & Nutrition*, 6(4), 736-746.
- Teeboonma, U., Tiansuwan, J. & Soponronnarit, S. (2003). Optimization of heat pump fruit dryers. *Journal of Food Engineering*, 59(4), 369-377.
- Tincheva, P. A. (2019). The effect of heating on the vitamin C content of selected vegetables. *World Journal of Advanced Research and Reviews*, 3(3), 27-32.
- Torki-Harchegani, M., Ghanbarian, D., Ghasemi Pirbalouti, A. & Sadeghi, M. (2016). Dehydration behaviour, mathematical modelling, energy efficiency and essential oil yield of peppermint leaves undergoing microwave and hot air treatments. *Renewable and Sustainable Energy Reviews*, 58, 407-418.
- Tuncal, C. & Doymaz, İ. (2020). Performance analysis and mathematical modelling of banana slices in a heat pump drying system. *Renewable Energy*, 150, 918-923.
- Xanthopoulos, G., Oikonomou, N. & Lambrinos, G. (2007). Applicability of a single-layer drying model to predict the drying rate of whole figs. *Journal of Food Engineering*, 81(3), 553-559.
- Yang, Z., Zhu, E., Zhu, Z., Wang, J. & Li S. (2013). A comparative study on intermittent heat pump drying process of Chinese cabbage (*Brassica campestris* L.ssp) seeds. *Food and Bioprocess Processing*. 91(4), 381-388.
- Zielinska, M., Zapotoczny, P., Alves-Filho, O., Eikevik, T. M. & Blaszcak, W. (2013). A multi-stage combined heat pump and microwave vacuum drying of green peas. *Journal of Food Engineering*, 115(3), 347-356.
- Zogzas, N. P., Maroulis, Z. B. & Marinos-Kouris, D. (1996). Moisture Diffusivity Data Compilation in Foodstuffs. *Drying Technology*, 14(10), 2225-2253.

## **BADANIE WŁAŚCIWOŚCI SUSZENIA, KOLORU ORAZ ZACHOWANIA WITAMINY C W PIASTRACH ZIEŁONEGO BANANA SUSZONYCH ZA POMOCĄ PRÓŻNIOWEJ POMPY CIEPŁA**

**Streszczenie.** Niniejsze badania miało na celu ocenę właściwości usuwania wilgoci z plasterów zielonego banana oraz wpływu warunków suszenia na kolor i zachowanie witaminy C w systemie suszenia przy pomocy próżniowej pompy ciepła. Plastry zielonego banana zostały poddane suszeniu w 40, 50 i 60 °C przy poziomach podciśnienia wynoszących 0,40 i 80 kPa. Średni czas suszenia zmniejszył się o 18,9 i 32,7% gdy podciśnienie i temperatura odpowiednio wzrosły. Sześć modeli o cienkich warstwach poddano ocenie w celu wyjaśnienia procesu kinetycznego, który towarzyszy procesowi usuwania wilgoci za pomocą próżniowej pompy ciepła ustawionej tak, aby zapewnić różnorodne okoliczności doświadczenia i dopasować ją do danych eksperymentalnych. Wyniki pokazały, że właściwości usuwania wilgoci z plasterów zielonego banana mogą być najdokładniej wyjaśnione przy pomocy modelu Page'a. Wystąpił wzrost efektywnej dyfuzji wilgoci, który wahał się w zakresie  $1,1658 \times 10^{-10}$  do  $1,9717 \times 10^{-10} \text{ m}^2 \cdot \text{s}^{-1}$ , ze wzrostem temperatury i podciśnienia. Energia aktywacji wahała się w zakresie od 15,99 do 19,73  $\text{kJ} \cdot \text{mol}^{-1}$  co zostało wyjaśnione wyrażeniem wykładniczym na podstawie Model Arrheniusa. Temperatura suszenia 50°C w podciśnieniu wynoszącym 80kPa było w stanie zachować witaminę C w 55, 9% co stanowi optymalne warunki suszenia do osiągnięcia wysokiej jakości produktu.

**Keywords:** cienkowarstwowy model suszenia, suszenie za pomocą próżniowej pompy ciepła, plastry zielonego banana, witamina C, poziom ekstrakcji wilgoci właściwej